Molecular Crystals and Liquid Crystals
Publication details, including instructions for authors and subscription information:
http://www.tandfonline.com/loi/gmcl16

Spin Dynamics in Disordered TCNQ Salts

Z. G. Soos [a] & S. R. Bondeson [b]
[a] Department of Chemistry, Princeton University
[b] Department of Chemistry, University of Wisconsin, Stevens Point

Version of record first published: 14 Oct 2011.

To cite this article: Z. G. Soos & S. R. Bondeson (1982): Spin Dynamics in Disordered TCNQ Salts, Molecular Crystals and Liquid Crystals, 85:1, 19-31

To link to this article: http://dx.doi.org/10.1080/00268948208073628

Mol. Cryst. Liq. Cryst., 1982, Vol. 85, pp. 19–31
0026-8941/82/8501-0019$06.50/0

Printed in the United States of America

(Proceedings of the International Conference on Low-Dimensional Conductors, Boulder, Colorado, August 1981)

SPIN DYNAMICS IN DISORDERED TCNQ SALTS

Z. G. Soos
Department of Chemistry
Princeton University

S. R. Bondeson
Department of Chemistry
University of Wisconsin, Stevens Point

Received for publication September 17, 1981

A segment model with $c \sim 0.10$ weak exchanges among 1-c strong exchanges accounts for the static thermodynamics of several structurally disordered, complex TCNQ salts. The segment model is extended to the spin dynamics of random-exchange Heisenberg antiferromagnetic chains (REHACs), as probed by magnetic resonance. The exchange-narrowed epr linewidth and resonance shifts at ultralow temperature are related to dipolar interactions among spins delocalized on parallel odd-length segments. REHACs display a wide variety of exchange fields and are thermally decoupled into finite domains. An inhomogeneous superposition of such finite domains is probed in magnetic resonance experiments.

I. RANDOM EXCHANGE HEISENBERG ANTIFERROMAGNETIC CHAINS

Low temperature power laws characterize the thermodynamics of random-exchange Heisenberg antiferromagnetic chains (REHACs). The basic Hamiltonian for $\vec{s}_n = \frac{1}{2}$ spins is

$$\mathcal{H}/J = \sum_n (2x_n \vec{s}_n \cdot \vec{s}_{n+1} + h s_{nz}) \qquad (1)$$

where J is the largest antiferromagnetic exchange, $0 \leq x_n \leq 1$ are independent random variables, and $h = g\mu_B H/J$ describes interactions with a static magnetic field H. A normalized distribution f(x) of the random exchanges then specifies

completely such static properties as the magnetic susceptibility $\chi(T)$, the magnetization $M(T,H)$, and the magnetic specific heat $C(T,H)$. Eq.(1) has primarily been applied[1,2] to structurally disordered, complex salts of TCNQ (tetracyanoquinodimethane) with asymmetric cations like quinolinium (Q^+), acridinium (Ad^+), etc. The s_n sites are associated with $(TCNQ)_2^-$ supermolecular radicals in $Q(TCNQ)_2$ and $Ad(TCNQ)_2$, whose REHAC power laws occur below 20K.

Clark and coworkers have reported[3-6,1] NMR and epr investigations of REHAC spin dynamics in $Q(TCNQ)_2$, including samples damaged by irradiation. Their analysis is necessarily phenomenological, since few properties of $\mathcal{H}_o$ are available. Magnetic resonance studies clearly require extensions of Eq.(1) to include hyperfine and three-dimensional dipolar interactions. Recent epr results[7] on $Q(TCNQ)_2$ at ultralow temperatures, 0.5 mk < T < 10 mK, indicate that $\chi(T)$ deviates from a REHAC power law. The concomitant development of a resonance shift cannot be associated with Eq. (1) since commuting with S_z precludes any shift.

We adopt here the previous approach, that magnetic terms are weak perturbations to $\mathcal{H}_o$ in Eq.(1), and discuss REHAC spin dynamics in terms of a segment model.[8] The microscopic picture of spins delocalized on odd-length segments, or an odd number of $(TCNQ)_2^-$ sites, differs in important ways from previous ideas about localized spins interacting with a singular distribution, $f_1(x) \sim x^{-\alpha}$ and $\alpha \sim 0.8$. Different renormalization approaches[9,10,8] show that a singular distribution is not required for power laws at low temperature. The almost flat $\chi(T)$ behavior in Fig. 1 for $Q(TCNQ)_2$ and $Ad(TCNQ)_2$ at T > 20K, on the other hand, indicates that most (90 $\pm$ 10%) of the exchanges are comparable. A segment of p+1 sites then corresponds to p successive comparable exchanges, with significantly weaker exchanges at both ends.

The normalized bimodal distribution[8] for the random exchanges

$$f_2(x) = c\delta(\varepsilon - x) + (1-c)\delta(1-x) \qquad (2)$$

is the simplest choice for concentrations c and 1-c, respectively, of weak exchanges εJ and strong exchanges J along the chain. The parameters $c = 0.10$, $\varepsilon = 0.30$, and $J/k = 230K$ fit[8] the available static thermodynamics of

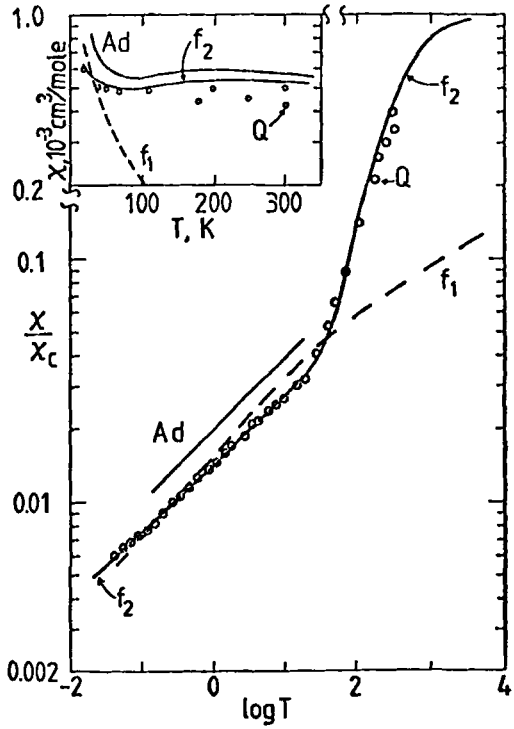

Fig. 1. Absolute $\chi(T)/\chi_c$ and (inset) $\chi(T)$ data for $Q(TCNQ)_2$ and for $Ad(TCNQ)_2$. The $f_2(x)$ fit for weakly interacting segments is based on $\varepsilon = 0.30$, $c = 0.10$, and $J = 230$ K. The singular distribution $f_1(x)$ has $\alpha = 0.75$ and $J = 2 \times 10^7$K. (ref. 8).

$Q(TCNQ)_2$ for $T \gtrsim 30$ mK, as shown for $\chi(T)$ in Fig. 1. The probability for a segment with p+1 sites is $c(1-c)^p$ for randomly distributed weak exchanges. The average length of segments is c^{-1}. The $Q(TCNQ)_2$ paramagnetism associated with the doublet ground state of odd segments is $c/(2-c) \sim 0.05$ spins per site. Thus c/2 can be estimated through the crossover around 20K in Fig. 1 from interacting odd segments to internal excitations of finite segments.

The preponderance of comparable nearest-neighbor exchanges J follows from $\chi(T)$ data. The physical motivation for segments has to do with the short-range order of asymmetric cations. Completely random up or down orientations for successive cations is hard to reconcile with elementary packing considerations. Occasional misoriented cations and considerable short-range order are consistent with structural data. A distribution of weak exchanges in the $(TCNQ)_2^-$ stacks may then reflect changes in the cationic orientations on one or more adjacent chains.

In contrast to the strong case for segments, the distribution of the weak exchanges remains open. The δ-function choice in Eq.(2) is particularly convenient. A singular distribution $x^{-\alpha}$ for the 10% weak exchanges is certainly possible. These weak interactions are inevitably obscured. For $kT > \varepsilon J$, the segments are thermally decoupled and the weak exchanges do not matter, while for $kT < \varepsilon J$ the internal excitations of segments are frozen out and renormalized interactions between odd segments dominate the thermodynamics. The renormalized exchanges[8] depend on the lengths of the odd segments and on the number and lengths of intervening diamagnetic even segments. Eq(2) gives a renormalized distribution[11] x^{δ}, with $\delta \sim 0.29$.

The low-temperature properties of finite segments thus yield[8] another REHAC, with renormalized exchanges x_n in Eq.(1) between $s = \frac{1}{2}$ spins for odd segments n and n±1 along the chain. Paramagnetic odd segments and diamagnetic even segments are interspersed. The resulting localized states have a wide distribution of internal fields and, as is typical for localized states in disordered systems, their physical properties involve inhomogeneous averages. We consider in Section II dipolar and hyperfine interactions among odd-length segments and summarize[11] in Section III the unusual temperature dependence of the exchange-narrowed epr linewidth of $Q(TCNQ)_2$ for $T \gtrsim 30mK$. Pairwise dipolar interactions are examined in Section IV in connection with ultralow temperatures. The discussion is always specialized to $Q(TCNQ)_2$ for estimates of interaction strengths.

II. PARAMAGNETISM OF ODD SEGMENTS

Antiferromagnetic exchanges reduce $\chi(T)$ from χ_c, the Curie law for noninteracting spins. The effective density of free spins per site,

$$n(T) = \chi(T)/\chi_c \leq 1 \qquad (3)$$

involves purely experimental quantities. It is exactly related, via the fluctuation-dissipation theorem, to the sum of all static correlations. We see from Fig. 1 that $n(20) \sim 4\%$, $n(1) \sim 1.4\%$, and $n(.001) \sim 2\times10^{-3}$ on exptrapolating. Most of the concentration $c/(2-c) \sim 0.05$ of odd segments are active at 20K. Greater spin dilution occurs at lower temperature as strongly interacting sequences of odd segments freeze out to $S = 0$ or $\frac{1}{2}$ for even and odd sequences,

respectively. Adjacent odd segments in Fig. 2 interact most strongly, then odd segments separated by one even segment, etc.

The dipolar second moment $M_2(T)$ of a dilute paramagnetic lattice is[12]

$$M_2(T) = n(T)M_2(\infty) \qquad (4)$$

where $M_2(\infty)$ is the usual high-temperature result. Diamagnetic Q^+ and paramagnetic $(TCNQ)_2^-$ molecular sites lead[11] roughly to $2\times10^4 G^2$ for $M_2(\infty)$. Dipolar fields then go as $n^{\frac{1}{2}}(T)$ and are of the order of 5G at 1mK. These estimates are not significantly changed on delocalizing the spin over c^{-1} sites in a segment.

Dipolar fields exceed the hyperfine interactions[13] of 0.7G for $(TCNQ)_2^-$ radicals, which decrease as $c^{\frac{1}{2}}$ on delocalizing over c^{-1} sites. Rather long odd segments, or odd sequences of odd segments, are still paramagnetic below 1K, where strong T and H dependences are observed[4] in the proton spin-lattice relaxation. Such small hyperfine fields are probed by NMR, but are relatively unimportant for epr.

Odd segments in the same chain are exchange coupled and adjacent odd segments in Fig. 2 are readily frozen out. Intrachain dipolar interactions are strongly suppressed. The strongest interaction, as shown in Fig. 3, between spins delocalized on segments L_1 and L_2 is evidently for over-

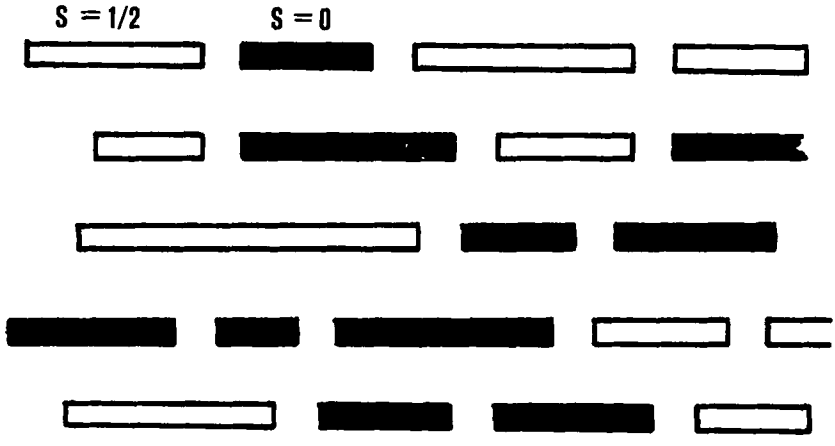

Fig. 2. Even and odd segments at low temperature.

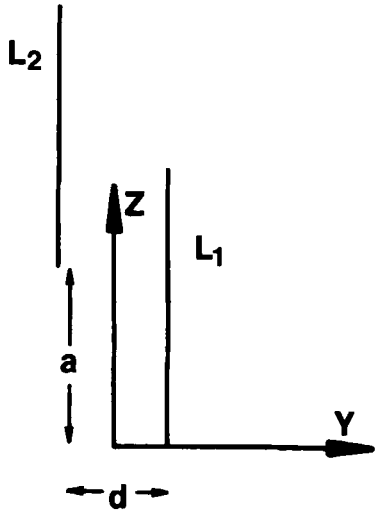

Fig. 3. Dipolar principal axes for spins delocalized on adjacent segments L_1 and L_2, for the case of strong overlap with a, d << L_1, L_2.

lapping (a << L_1, L_2) adjacent chains. To lowest order in L_1^{-1}, L_2^{-1} the dipolar principal axes (X,Y,Z) of such pairs coincide and the zero-field Hamiltonian[14] is

$$\mathcal{H}_D = E(S_X^2 - S_Y^2) \tag{5}$$

The fine-structure constant E is, again to lowest order in L_1^{-1}, L_2^{-1},

$$E = \frac{g^2\mu_B^2}{2}\ \frac{1}{r^3} \sim \frac{g^2\mu_B^2}{2}\ \frac{(L_1 + L_2)}{d^2 L_1 L_2} \tag{6}$$

An interchain separation of d $\sim$ 5Å and $L_1 \sim L_2 \sim$50Å yields E $\sim$ 10G. Some dimers are consequently strongly coupled. The mean square amplitude of E over all active odd segments is essentially $M_2(T)$.

Exchange narrowing requires a modulation, ω_e, that exceeds internal dipolar fields. Linear chains and REHACs have additional complications. The general point is that the renormalized exchanges x_n in Eq. (1) decrease rapidly as odd segments are frozen out. Interchain dipolar interactions among surviving moments, on the other hand, decrease only to the extent that L_1 and L_2 increase. The modulation ω_e thus eventually fails to average all dipolar fields and

isolated paramagnetic clusters are formed at very low temperature. We have a percolation problem for partitioning active spins into dimers or exchange-coupled aggregates.

Complex TCNQ salts have 4-6 nearest-neighbor TCNQ stacks. Each segment in Fig. 2 has around two adjacent segments, either even or odd, per adjacent chain. Some 10% of the odd segments are active at $T \sim 10$ mK, $n \sim 5\times10^{-3}$ in $Q(TCNQ)_2$, when there is about one adjacent odd segment per active spin. The powder average of Eq. (5) for decoupled dimers is examined below for the ultralow temperature resonance shift.

III. EXCHANGE NARROWING

The localized spin states in REHACs are thermally decoupled whenever kT exceeds the exchange. The resulting domains must be treated separately, leading to inhomogeneous averages. We summarize here such an approach[11] to the exchange-narrowed epr linewidth of $Q(TCNQ)_2$ for $T > 30$ mK. Direct analysis[8] of replicas based on 10 odd segments, or about 20 $c^{-1} \sim 200$ sites of the original lattice, yield the static thermodynamics and include[11] all effective exchanges of 30 mK or more. The strong, or intrachain, exchange modulation of 10-segment replicas is thus appropriate for $T \geq 30$ mK. These random exchanges x_n, with n = 1, 2, ...9, are readily generated for chains of segments and vary enormously in the 100 replicas used for the thermodynamics.

Our explicit approximation for $x_k(T)$, the effective intrachain exchange in the kth replica, is[11]

$$x_k(T) = N^{-1}\sum_n x_n \exp(-\beta x_n) \qquad (7)$$

where $\beta = J/kT = 230/T$, N = 10, and x_n are the 9 renormalized exchanges between successive odd segments plus a smaller exchange of 9×10^{-4} to the next replica. The intrachain modulation ω_k is taken as $\hbar\omega_k = 2Jx_k(T)$. Its temperature dependence in Eq. (7) is largely controlled by the x_n for interacting odd segments.

$Q(TCNQ)_2$ has two magnetically inequivalent $(TCNQ)_2^-$ chains, which however yield a narrow average epr line even at high field.[3] Interchain interactions larger than dipolar are needed. We postulate a transverse exchange field $\omega_\perp$ with the same temperature dependence, $n^2(T)A$, and take $A = 2\times10^4$G. Such a transverse cutoff produces

a Lorentzian resonance[15] with a half-width of

$$\Gamma_k(T) = M_2(T)[2\omega_k(T)\omega_\perp(T)]^{-\frac{1}{2}} \qquad (8)$$

for the kth replica. Similar crystalline environments are assumed for all replicas, with $M_2(\infty) = 10^4G^2$ and a common tranverse cutoff, while the intrachain exchange $\omega_k(T)$ varies strongly from one replica to the next.

The paramagnetism $\chi_k(T)$ of the kth replica, which is already known from the $\chi(T)$ calculation for Fig. 1, corresponds to the epr intensity. These intensities are readily distributed in Lorentzians with half-widths $\Gamma_k(T)$. The resulting sum of 100 Lorentzians remains nearly Lorentzian and has a width $2\Gamma(T)$ shown in Fig. 4. The exchange-narrowed REHAC resonance has an unusual, approximately logarithmic temperature dependence that results primarily from the

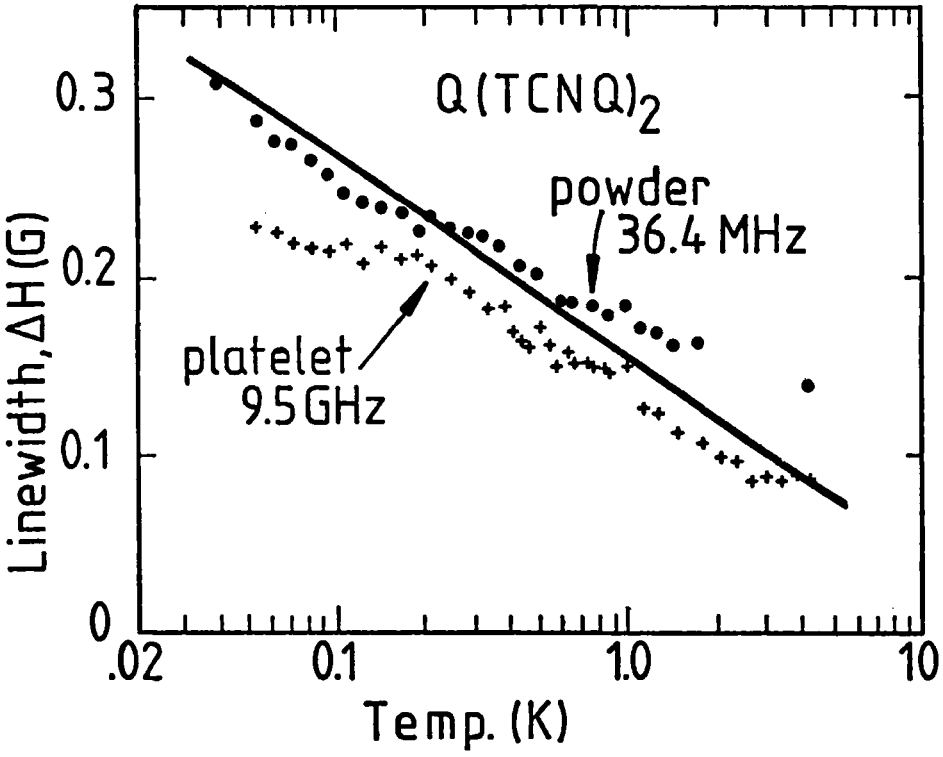

Fig. 4. Width at half-height of the $Q(TCNQ)_2$ epr absorption, from ref. 3. The solid line, from ref. 11, is based on parameters cited in the text.

imhomogeneous sum over replicas, which explicitly correlate the intensity $\chi_k(T)$ and exchanges $x_k(T)$ within thermally-decoupled domains.

The upturn of the epr linewidth in $Q(TCNQ)_2$ above 10K coincides with the crossover from interacting segments to internal excitations of segments. REHAC power laws are restricted to the former. The roughly constant $Q(TCNQ)_2$ linewidth above 20K represents typical, but far from completely understood, epr absorptions in ion-radical organic solids.[2] Both the one-dimensionality and the large intrachain exchanges are general complications whose treatment is no easier in REHACs.

IV. ULTRALOW TEMPERATURES

The linewidth Γ_k in Eq. (8) is, in effect, the internal field in the kth domain when the modulation ω_k exceeds the dipolar internal fields. A Lorentzian epr absorption at the Larmor frequency is expected for $g\mu_B H_o/J = h_o >> \Gamma_k$. Cooling slows the modulation and reduces the number of spins, n(T). When the dipolar interaction E, in Eq. (5), between nearby segments in adjacent chains exceeds $\omega_k(T)$, the segments are not exchange narrowed but must be treated separately. The $T \to 0$ limit reduces to decoupled clusters that we approximate here as dimers with a normalized distribution g(E) of zero-field splittings. The previous estimates of E rationalize the crossover in the 10 mK range, but the partitioning of spins to dimers and exchange-narrowed aggregates remains open. The REHAC topology in $Q(TCNQ)_2$ leads to common principal axes for $\mathcal{H}_D$ in Eq. (5), as shown in Fig. 3.

In a large applied field $h >> E$, the Zeeman levels of a dimer are nearly exact. The epr spectrum is centered on h_o and has fine-structure splitting of the order of E, depending on the orientation of $\vec{h}$ in X, Y, Z. The powder average for a distribution g(E) gives a width of approximately

$$2\bar{E} \simeq 2\int_0^\infty Eg(E)dE \qquad (9)$$

Only the $\Delta M_S = \pm 1$ transitions contribute in the high-field limit.

The situation is quite different for $h \sim E$. Now $\mathcal{H}_D + \vec{h}\cdot\vec{S}$ leads to a 3x3 matrix[15] whose eigenvalues are roots of

$$\lambda^3 - (E^2 + h^2)\lambda + E(h_x^2 - h_y^2) = 0 \qquad (10)$$

These are shown in Fig 5a for orientations of $\vec{h}$ such that $h_x^2 = h_y^2$, when Eq (10) is easily solved. The situation for other orientations is shown schematically in Fig. 5b. The two zero-field transitions at E and the transition at 2E all have equal intensities at h = 0. As h increases, the half-field transition loses intensity roughly as E^2/h^2. We are computing the powder average of the epr spectrum for dimers with an assumed distribution g(E) of zero-field splittings.

The ultralow temperature results[7] indicate an internal field of about 3G, independent of the resonance field h_o between about 4 - 9G. The zero-field splittings must clearly be included explicitly, since $\bar{E} \sim$ 1-3G is indicated. About half of the unit sphere has $|h_x| \sim |h_y|$, when the energies in Fig. 5a show the $\Delta M = 1$ transitions to occur at lower fields, $(h_o^2 - E^2)^{1/2}$, while the $\Delta M = 2$ transition is

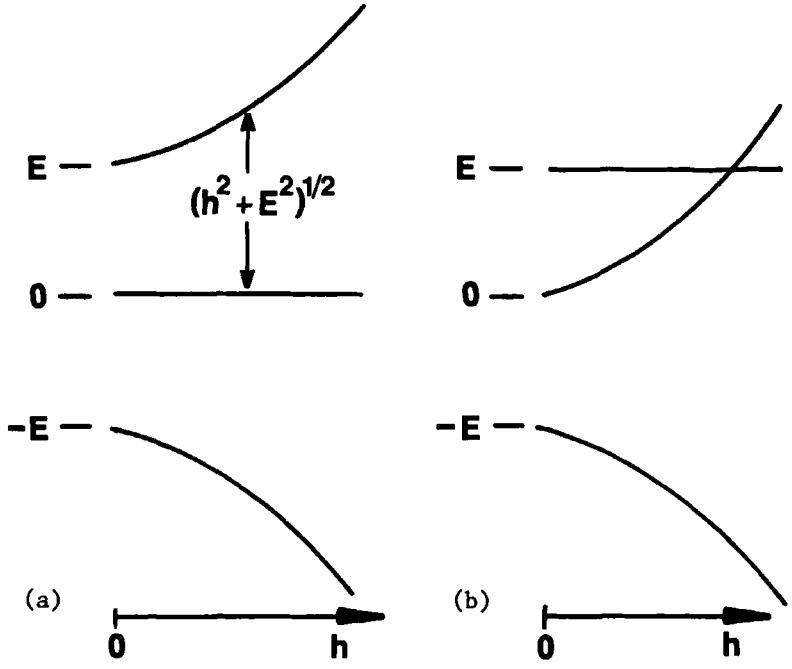

Fig. 5. Energy levels of dipolar dimers in a magnetic field.

at $\frac{1}{2}(h_o^2 - 4E^2)^{\frac{1}{2}}$. The entire spectrum for these orientations lies in $0 < h < h_o$. Examination of other orientations confirms that the resonance is shifted to lower field, but it remains to be seen from a powder average whether the shift is in fact independent of h_o. We note that $\mathcal{H}_D$ in Eq. (5) reflects directly the model of spins delocalized on segments, rather than localized on sites.

The formation of dimers also changes $\chi(T)$. The energies in Fig. 5 must be augmented by the singlet state, which is at zero in the absence of any interchain exchange and is lowered by 2J' for an AF coupling. Even J' = 0 leads to a reduced $\chi(T)$, but only for kT < E. The observed reductions[7] probably involve finite J' and a crossover to small clusters. These consequences of zero-field splittings require additional work.

V. DISCUSSION

Sequences of odd segments result in a wide variety of spin densities, $\rho_n(T)$, along the chain. The hyperfine interaction $a\rho_n$, with $a \approx 0.7$G for $(TCNQ)_2^-$ radicals, provides a spin-lattice relaxation mechanism. Proton T_1^{-1} data[4] in $Q(TCNQ)_2$ show strong T and H dependences below 1K. These results, which have yet to be interpreted, provide additional applications of the segment model.

As usual in paramagnetic organic solids[2], the protons are sufficient strongly coupled to have a single decay time, even for protons at diamagnetic Q^+ sites or in even segments. The motion and relaxation of the electronic moments are the rate limiting step for T_1^{-1}. Since there are few phonons below 1K, energy conservation in I^+S^- or I^-S^+ processes requires degenerate electronic states with $\hbar\omega_N$, the small nuclear Zeeman energy. The REHAC density of spin-flip states is then proportional to T_1^{-1}, as shown[16] in low fields for the regular Heisenberg chains of α-CuNSal. The distribution of exchanges between odd segments suppresses a sharp critical field, but T_1^{-1} nevertheless decreases with increasing H.

The excitations of Eq. 1, even for uniform x_n, are neither fermions nor bosons. Their complicated statistics are modeled, as in α-CuNSal, by transforming to interacting fermions[17,16] that correspond to spin flips. The Fermi energy is related to S_z and thus depends on the applied field. Localized states in REHACs clearly differ from regular chains. Furthermore, thermal decoupling points to local densities of states. For T > 30mK we are again taking replicas of 10 odd

segments, or 10 fermions. The best energies for noninteracting fermions are found, at any T, by comparing with the static thermodynamics.

We have sketched above an approach to spin dynamics in REHACs. Many additional comparisons, as well as more complete analyses, will be needed to establish a consistent picture. Several general points have already emerged from the segment model. First, the magnetic properties of REHACs like $Q(TCNQ)_2$ have a crossover from interacting odd segments at low temperature to excitations of finite segments. Second, both static and dynamic properties at low temperature reflect widely different effective exchanges between odd segments in thermally decoupled sequences. Third, conventional treatments of dipolar and hyperfine interactions, of one-dimensional effects, and of transverse cutoffs are possible in REHACs, once their local distributions are introduced. The strong T and H dependences in REHACs then facilitate comparison with general theories. Finally, at ultralow temperature we expect small dipolar clusters, with characteristic principal axes for parallel odd segments, as the effective exchanges become very small.

We gratefully acknowledge support for this work through NSF-DMR-7727418 A01.

REFERENCES

1. W. G. Clark, in Physics in One Dimension (ed. J. Bernasconi and W. Schneider, Springer-Verlag, Berlin, 1981) p. 289.
2. Z. G. Soos and S. R. Bondeson, in Extended Linear Chain Compounds, Vol. 3 (ed. J. S. Miller, Plenum, New York) in press.
3. J. Sanny and W. G. Clark, Solid State Commun. 35, 473 (1980).
4. L. J. Azevedo, W. G. Clark, E. O. McLean, and P. L. Seligman, Solid State Commun. 16, 1267 (1975).
5. J. Sanny, G. Grüner, and W. G. Clark, Solid State Commun. 35, 657 (1980).
6. L. C. Tippie and W. G. Clark, Phys. Rev. B23, 5854(1981).
7. H. M. Bozler, C. M. Gould, and W. G. Clark, Phys. Rev. Lett. 45, 1303 (1980).
8. S. R. Bondeson and Z. G. Soos, Phys. Rev. B22, 1793 (1980); Solid State Commun. 35, 11 (1980).
9. S. Ma, C. Dasgupta, and C. K. Hu, Phys. Rev. Lett. 43, 1434 (1979); C. Dasgupta and S. Ma, Phys. Rev. B22, 1305 (1980).

10. J. E. Hirsch and J. V. José, J. Phys. C. Lett. 13, L53 (1980); Phys. Rev. B22, 5339 (1980).
11. Z. G. Soos and S. R. Bondeson, Solid State Commun. 39, 289 (1981).
12. Z. G. Soos, J. Chem. Phys. 46, 4284 (1967); 49, 2493 (1968).
13. P. I. Kuindersma, G. A. Sawatzky, and J. Kommandeur, J. Phys. C. 8, 3008, 3016 (1975).
14. A. Carrington and A. D. McLachlan, Introduction to Magnetic Resonance (Harper and Row, New York, 1967) Ch. 8.
15. Z. G. Soos, J. Chem. Phys. 44, 1729 (1966).
16. L. J. Azevedo, A. Narath, P. M. Richards, and Z. G. Soos, Phys. Rev. B21, 2871 (1980); Phys. Rev. Lett. 43, 875(1979).
17. L. N. Bulaevskii, Sov. Phys. JETP 16, 685 (1963).